

# $\gamma$ -ray and ultra-high energy neutrino background suppression due to solar radiation

Shyam Balaji<sup>1,\*</sup>

<sup>1</sup>*Laboratoire de Physique Théorique et Hautes Energies (LPTHE),  
UMR 7589 CNRS & Sorbonne Université, 4 Place Jussieu, F-75252, Paris, France*

The Sun emits copious amounts of photons and neutrinos in an approximately spatially isotropic distribution. Diffuse  $\gamma$ -rays and ultra-high energy (UHE) neutrinos from extragalactic sources may subsequently interact and annihilate with the emitted solar photons and neutrinos respectively. This will in turn induce an anisotropy in the cosmic ray background due to attenuation of the  $\gamma$ -ray and UHE neutrino flux by the solar radiation. Measuring this reduction, therefore, presents a simple and powerful astrophysical probe of electroweak interactions. In this letter we compute such anisotropies, which at the Earth (Sun) can be  $\simeq 2 \times 10^{-3}$  (0.5)% and  $\simeq 1 \times 10^{-16}$  ( $2 \times 10^{-14}$ )% for TeV scale  $\gamma$ -rays and PeV scale UHE neutrinos respectively. We briefly discuss exciting observational prospects for experiments such as the Fermi Gamma-Ray Space Telescope Large Area Telescope (Fermi LAT), High Energy Stereoscopic System (H.E.S.S.), High-Altitude Water Cherenkov (HAWC) detector and IceCube. The potential for measuring  $\gamma$ -ray attenuation at orbital locations of other active satellites such as the Parker Solar Probe and James Webb Space Telescope is also explored.

## I. INTRODUCTION

The extragalactic background is a superposition of all radiation sources, both individual and diffuse, from the edge of the Milky Way to the edge of the observable universe, and is thus expected to encode a wide range of phenomena [1, 2]. It is broadly comprised of electromagnetic radiation and neutrinos which have a characteristic energy density and spectrum. Contributions are guaranteed from established extragalactic -ray source classes such as active-galactic-nuclei (AGN), star-forming galaxies, and  $\gamma$ -ray bursts [3]. It provides a non-thermal perspective on the cosmos, which is also explored by the cosmic radio background, extragalactic cosmic rays (CRs), and neutrinos.

The electromagnetic component often referred to as the extragalactic background light (EBL) is the total integrated flux of all photon emission over cosmic time [4–6]. This EBL is dominated energetically by thermal relic radiation from the last scattering surface observed as the cosmic microwave background (CMB). Different physical processes characterize the EBL in each waveband: starlight in the optical, thermal dust emission in the infrared, and X-ray emission from AGN [7].

Similarly, for neutrinos, the high energy frontier is expected to be especially rich, with neutrinos from baryonic accelerators ( $\gamma$ -ray bursts, AGN, etc.) extending up to about  $\simeq 100$  GeV [8]. At even higher energies, the ultra-high energy (UHE) regime will exhibit cosmogenic neutrinos and may even reveal the presence of topological defects, which could emit neutrinos via a variety of energy loss channels [8]. For sources far beyond the gamma ray horizon, neutrinos may be the only probe because, even at the highest energies, they propagate freely up to cosmological distances. The observation of UHE particles such as photons, ions, and neutrinos provides critical information on astrophysical systems as well as the mechanisms of charged particle acceleration in these systems.

Since there is significant contamination from foregrounds, direct measurements of the EBL and neutrino background are difficult, necessitating the use of indirect observational or theoretical determinations to obtain an estimate of emitter populations [9]. Exotic contributions, such as those resulting from a possible connection between dark matter and Standard Model (SM) particles, may be present in addition to astrophysical emissions. This possibility was recently considered in Ref. [10].

The interaction between the CMB and the cosmic neutrino backgrounds with  $\gamma$ -rays and UHE neutrinos and the subsequent CR anisotropies have been studied in detail [11–15]. Here, we will focus on a qualitatively different phenomena, computing instead the local anisotropy in the  $\gamma$ -ray and UHE neutrino background due to photon and neutrino emission from the Sun. A simple attempt at estimating the extinction of  $\gamma$ -rays due to sunlight was made in Ref. [16]. However the blackbody energy spectrum of the Sun was not included and the optical depth was estimated locally instead of being integrated over the entire region of the solar system where the sunlight and  $\gamma$ -rays are interacting. Additionally, the optical depth as a function of  $\gamma$ -ray energy was not studied.

Here, we will include these effects and also consider the neutrino analogue whereby solar neutrinos annihilate with UHE antineutrinos or vice versa. We discuss the prospects for measuring the predicted  $\gamma$ -ray anisotropies with both space and ground-based experiments such as the Fermi Gamma-Ray Space Telescope Large Area Telescope (Fermi LAT), High Energy Stereoscopic System (H.E.S.S.) as well as the High-Altitude Water Cherenkov (HAWC) experiment. We then discuss the possibility of measuring UHE neutrino anisotropies with the IceCube experiment. We also predict the expected attenuation at the Parker Solar Probe and James Webb Space Telescope (JWST) orbits and review the possibility of measuring EBL suppression due to the Sun at these locations in the future. Complete understanding of these anisotropies

within the SM will enable constraints on beyond the SM models containing new states that could cause attenuation of the EBL or UHE neutrino background. In this letter, we will first outline the photon-photon and neutrino-antineutrino annihilation cross sections, then compute the optical depths and finally discuss experimental consequences. We will use natural units (where  $\hbar = c = k_B = 1$ ).

## II. ANNIHILATION PROCESSES

### Cross sections

We will first consider the cross section for two photons annihilating into an electron-positron pair. For a  $\gamma$ -ray with energy  $E_\gamma$ , the annihilation cross section for the process  $\gamma\gamma \rightarrow e^+e^-$  [17–19] with a solar photon  $\gamma_\odot$  of energy  $E_{\gamma_\odot}$  is given by

$$\sigma_{\gamma\gamma}(\beta) = \frac{3\sigma_T}{16} (1 - \beta^2) \times \left[ 2\beta(\beta^2 - 2) + (3 - \beta^4) \log\left(\frac{1 + \beta}{1 - \beta}\right) \right], \quad (1)$$

where  $\sigma_T = \frac{8\pi}{3} \left(\frac{\alpha}{m_e}\right)^2 = 6.652 \times 10^{-25} \text{cm}^2$  is the Thomson scattering cross section,  $\alpha$  is the fine structure constant,  $m_e$  is the electron mass and a dimensionless kinematic factor is defined  $\beta = \sqrt{1 - E_{\text{th}}/E_\gamma}$ . Where the threshold energy for electron-positron pair production is given by

$$E_{\text{th}} = \frac{2m_e^2}{E_{\gamma_\odot}(1 - \cos\theta)}. \quad (2)$$

In this expression  $\theta$  refers to the scattering angle between the  $\gamma$ -ray and the solar photon. The threshold energy of the incident  $\gamma$ -ray for this process to occur when annihilating with a photon of energy  $E_{\gamma_\odot} \simeq 0.5 \text{ eV}$  (like the effective temperature of the Sun) is at least  $\simeq 0.5 \text{ TeV}$ . Note that we will not consider higher order processes such as  $\gamma\gamma \rightarrow e^+e^-e^+e^-$  since at high energy, the cross section approaches a relatively constant  $6.5 \mu\text{b}$  [20] which is much lower than the leading order process unless  $E_\gamma \gtrsim 10^8 \text{ TeV}$ . Annihilation of photons into other final states such as  $\mu^+\mu^-$  or  $\pi^+\pi^-$  are subdominant at the scales of interest in this work.

For the neutrino channel, the resonant neutrino-antineutrino annihilation into a fermion-antifermion,  $\nu\bar{\nu} \rightarrow Z^0 \rightarrow f\bar{f}$  occurs via the  $s$ -channel. It has Breit-Wigner shape and can be written [8, 11]

$$\sigma_{\nu\bar{\nu}}^R(p, k) = \frac{G_F \Gamma m_Z}{2\sqrt{2}k^2 p E_{\nu_\odot}} \int_{s_-}^{s_+} \frac{s(s - 2m_\nu^2)}{(s - m_Z^2)^2 + \xi s^2} ds, \quad (3)$$

where the Fermi constant is  $G_F = 1.16637 \times 10^{-5} \text{GeV}^{-2}$  [21]. The light neutrino mass is set to  $m_\nu = 0.08 \text{ eV}$

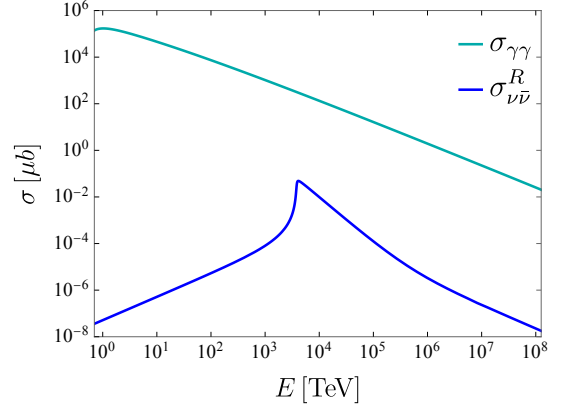


FIG. 1. Annihilation cross sections in units of  $\mu\text{b}$  for  $\gamma\gamma$  (cyan) and resonant  $\nu\bar{\nu}$  (blue) as function of the incident  $\gamma$ -ray or ultra-high energy neutrino respectively. We take  $E_{\gamma_\odot} = 0.5 \text{ eV}$  and  $E_{\nu_\odot} = 0.53 \text{ MeV}$  since these are typical energies for photons and neutrinos being emitted by the Sun.

and we define a dimensionless ratio  $\xi = \Gamma^2/m_Z^2$ , where  $\Gamma = 2.495 \text{ GeV}$  is the decay width of the  $Z$  boson with mass  $m_Z = 91.1876 \text{ GeV}$  [21]. The UHE neutrino has 4-momentum  $k^\mu = (E_\nu, \mathbf{k})$  while the solar neutrinos have  $p^\mu = (E_{\nu_\odot}, \mathbf{p})$ , hence it follows from the usual relativistic energy-momentum relation that  $k = \sqrt{E_\nu^2 - m_\nu^2}$  and  $p = \sqrt{E_{\nu_\odot}^2 - m_\nu^2}$ . The centre-of-mass energy is  $s = (p^\mu + k^\mu)^2 \simeq 2m_\nu^2 + 2\mathbf{k} \cdot (E_{\nu_\odot} \pm \mathbf{p})$  since  $E_\nu \simeq k$  at high energy. Also, we have  $\mathbf{k} \cdot \mathbf{p} = pk \cos\theta$ . Hence the integration limits in Eq. (3) are defined  $s_\pm = 2m_\nu^2 + 2k(E_{\nu_\odot} \pm p)$  corresponding to  $\theta = 0$  and  $\theta = \pi$  respectively.

We plot the resulting cross sections for photon-photon and resonant neutrino-antineutrino annihilation as a function of the incident cosmic ray particle energy in Fig. 1. We fix  $E_{\gamma_\odot} = 0.5 \text{ eV}$  and  $E_{\nu_\odot} = 0.53 \text{ MeV}$  respectively since these are the typical energies of photons and neutrinos being emitted from the Sun. The maximal cross section of  $\sigma_{\gamma\gamma} \simeq 1.7 \times 10^5 \mu\text{b}$  for  $\gamma\gamma$  occurs at  $E_\gamma \simeq 1 \text{ TeV}$  while for  $\nu\bar{\nu}$  it occurs at  $E_\nu \simeq 4 \times 10^3 \text{ TeV}$  at  $\sigma_{\nu\bar{\nu}}^R \simeq 4.8 \times 10^{-2} \mu\text{b}$ .

There are also non-resonant contributions, which include several other channels with final states such as  $\nu\nu \rightarrow \nu\bar{\nu}, l\bar{l}, WW, ZZ$  and  $Zh$  [22, 23], which we can approximate in total as in Ref. [12] with

$$\sigma_{\nu\bar{\nu}}^{NR} \simeq \frac{\sigma_{\nu\bar{\nu}}^{he}}{1 + E_r/E}, \quad (4)$$

where  $E_r = \frac{m_Z^2}{2m_\nu}$  and  $\sigma_{\nu\bar{\nu}}^{he} = 8.3 \times 10^{-4} \mu\text{b}$ . This is significantly smaller than the resonant contribution below  $E_{\text{th}}$  so we can safely omit these contributions when considering UHE neutrino scattering in the regime of interest.

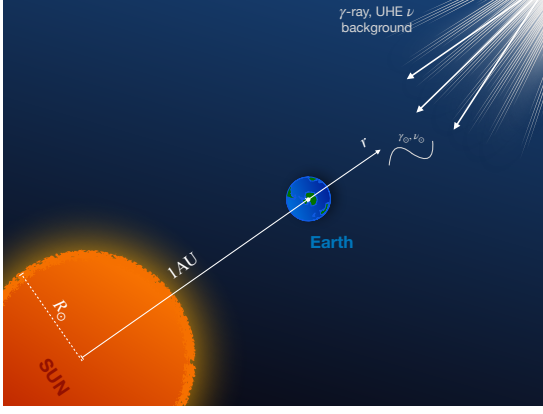


FIG. 2. Representation of coordinate system showing radial variable  $r$  where the extragalactic background photons and neutrinos interact with solar photons  $\gamma_\odot$  and neutrinos  $\nu_\odot$ .  $r'$  is the position at which we want to compute observable optical depth.

### Optical depth

The radiation spectrum of the Sun can be approximated as a blackbody. The peak wavelength is around 500 nm. In natural units, we get the differential luminosity per unit energy to be

$$\frac{dL_\odot}{dE_{\gamma_\odot}} = \frac{R_\odot^2}{E_{\gamma_\odot}^5 e^{E_{\gamma_\odot}/T_{\text{eff}}} - 1}, \quad (5)$$

where  $T_{\text{eff}} = 5780$  K is the effective blackbody temperature of the Sun [24] and  $R_\odot$  is the solar radius. We can show a visual representation of the Sun-Earth-EBL(UHE  $\nu$ ) system in Fig. 2. From here we can easily compute the differential photon number density per unit energy of the Sun at a distance  $r$  from the solar core with

$$\frac{dn_{\gamma_\odot}}{dE_{\gamma_\odot}} = \frac{1}{4\pi r^2} \frac{dL_\odot}{dE_{\gamma_\odot}}. \quad (6)$$

Note that there is an additional factor of  $c$  in the denominator which is omitted since  $c = 1$  in natural units.

From here we may now turn our attention to calculating the optical depth associated with a CR photon travelling an arbitrary distance through a background of sunlight. The differential optical depth per unit energy is given

$$\frac{d\tau_\gamma}{dE_{\gamma_\odot}} = \int_{r'}^\infty \frac{dn_{\gamma_\odot}}{dE_{\gamma_\odot}} \sigma_{\gamma\gamma}(E_\gamma, E_{\gamma_\odot}, \theta) dr, \quad (7)$$

where we use (1) for  $\sigma_{\gamma\gamma}$  and  $r'$  is the radial position at which we want to determine the  $\gamma$ -ray optical depth. Integrating over the solar photon energy to obtain the optical depth

$$\tau_\gamma = \int_{T_{\text{eff}}}^\infty \frac{d\tau}{dE_{\gamma_\odot}} dE_{\gamma_\odot}. \quad (8)$$

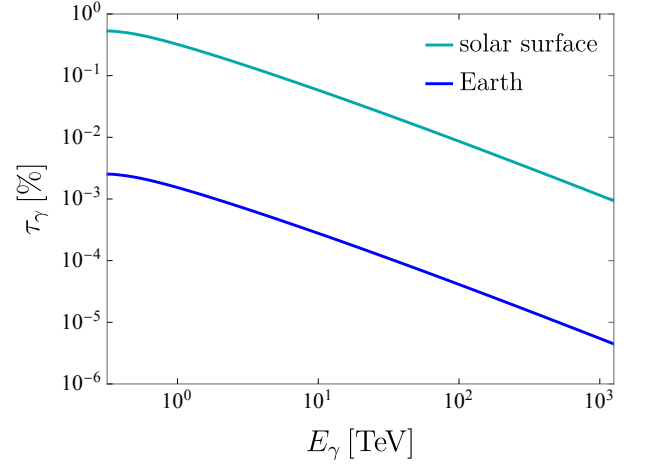


FIG. 3. Percentage optical depth  $\tau$  shown as a function of incident  $\gamma$ -ray energy in TeV. We show two scenarios, one is at the solar surface  $r' = R_\odot$  (cyan) and the other is at Earth  $r' = 1$  AU (blue). In both cases we take a scattering angle of  $\theta = \pi$ .

We may now plot the resulting optical depth due to the annihilation process as shown in Fig. 3. We show the optical depth at the solar surface and at Earth in cyan and blue respectively. The maximal optical depth is around the threshold energy at a scattering angle of  $\theta = \pm\pi$ . In the first case, the  $\gamma$ -ray photons must traverse through the sunlight till the surface of the Sun and in the second, the  $\gamma$ -ray must travel through a much lower number density of solar photons from beyond the Earth and Sun towards the Earth's surface. Unsurprisingly, of the two scenarios shown, the optical depth is maximised at the solar surface at around  $\tau_\gamma = 0.5\%$  since the  $\gamma$ -rays interact with a much larger number density of photons in this region. At Earth, the optical depth is maximised around  $\tau_\gamma = 2 \times 10^{-3}\%$ . In Ref. [16], the optical depth is estimated at 7% at the solar surface and  $3.3 \times 10^{-2}\%$  at the Earth. In both cases, the estimate is about an order of magnitude larger than what we obtain here. This is unsurprising since the energy distribution and radial dependence of the solar photons was not included or integrated over like here.

For UHE neutrino annihilation, we first require the solar neutrino luminosity which can be approximated  $L_{\nu_\odot} = 0.023L_\odot$  where  $L_\odot \simeq 4 \times 10^{33}$  erg/s is the total luminosity of the Sun [25]. We can approximate the neutrino number density at a distance  $r$  with

$$n_{\nu_\odot}(r) = \frac{1}{4\pi r^2} \frac{L_{\nu_\odot}}{\bar{E}_{\nu_\odot}}, \quad (9)$$

taking  $\bar{E}_{\nu_\odot} = 0.53$  MeV as the average neutrino energy emitted by the Sun [25]. Now we may compute the approximate optical depth  $\tau_\nu$ , for a high energy neutrino incident upon a solar neutrino

$$\tau_\nu = \int_{r'}^\infty n_{\nu_\odot}(r) \sigma_{\nu\bar{\nu}} dr, \quad (10)$$

using the maximum resonant neutrino annihilation cross section (at 4 PeV from Fig. 1 and Eq. (3)), we get  $\tau_\nu = 1 \times 10^{-16}\%$  at Earth and  $2 \times 10^{-14}\%$  at the solar surface.

### III. RESULTS AND DISCUSSION

Considering the Fermi LAT experiment [26], we see that the highest energy bin is 580-820 GeV. The reported intensity for this bin is  $\simeq 9.7 \times 10^{-12} \text{ cm}^{-2} \text{ s}^{-1} \text{ sr}^{-1}$ . If we consider that the intensity will be similar at 1 TeV, then we may multiply by the operating time of 1239 days, the angular coverage of 2.4 sr and an effective area of 8000  $\text{cm}^2$  [26] to get 20  $\gamma$ -ray events. Multiplied with the optical depth at Earth from Section II, we get a reduction of  $\simeq 3 \times 10^{-4}$  events. This is substantially below unity, so unless there is a factor of  $\simeq 10^4$  improvement in event count, it's unlikely that Fermi LAT will be able to probe such a tiny anisotropy.

If instead, we consider the H.E.S.S. experiment as in Ref. [27], we see from their Fig. A3 that one expects approximately  $\simeq 2.5 \times 10^4$   $\gamma$ -ray events at an energy of 1 TeV. Thus, multiplying with the optical depth at Earth, we get an isotropy of  $\simeq 0.4$  events over the data considered and assuming no large statistical fluctuations or other sources of significant background. This means that with just a factor of three increase in statistics, there would be a discernable integer event level anisotropy induced in the EBL.

Similarly, we can inspect the HAWC experiment data from 2014-2017 as in Ref. [28]. Studying the background classified events with  $\gamma$ -hadron cuts applied as shown in the blue dashed-line in Fig. 3 of Ref. [28] to ensure only events from the isotropic EBL and not from  $\gamma$ -ray interactions with the solar disk are counted. We see that the first bin of data has a median energy of 0.88 TeV while the second has 1.36 TeV, they contain  $\simeq 6.3 \times 10^6$  and  $\simeq 1.5 \times 10^6$  events respectively. Since  $E_\gamma = 1$  TeV lies between 0.88 TeV and 1.36 TeV, the event yield in this region can be estimated to be  $1.5\text{-}6.3 \times 10^6$ . Multiplying again by the optical depth at Earth from Section II we get a very noticeable  $\simeq 40\text{-}100$   $\gamma$ -ray events being attenuated. These anisotropies are significant and could very easily be tested in detail by HAWC. As HAWC continues to collect data, we can expect even better resolution of this EBL suppression.

For an instructive comparison, we may examine the dipole anisotropy measured by the Cosmic Background Explorer (COBE). This variation of  $\simeq 0.12\%$  results from the Earth's orbital motion about the Solar system barycenter and strikingly lies between the EBL optical depths evaluated at the solar surface and Earth respectively [29]. More recently, an all-sky measurement of the anisotropy induced by CRs travelling through our local interstellar medium and the interaction between the interstellar and heliospheric magnetic fields was performed [30]. The

analysis was based on data collected by the HAWC and IceCube observatories in the northern and southern hemispheres at the same median primary particle energy of 10 TeV. The horizontal anisotropy was measured to be  $\simeq 10^{-2}\%$ . This is comparable to the optical depth we compute at the Earth's surface. Furthermore, HAWC collected  $7.1 \times 10^{10}$  events with CRs of median energy 2 TeV between  $0.4\text{-}0.8^\circ$  [30] in an all-sky measurement of the anisotropy of cosmic rays. This was not limited to the EBL. We calculate the optical depth at the Earth's surface for a 2 TeV photon to be  $9.5 \times 10^{-6}$ . Hence, we would expect the attenuation due to sunlight at 2 TeV to be  $N_{\text{events}} \tau_\gamma \simeq 6.75 \times 10^5$  events. This seems very promising, however, these event counts correspond to CRs that are not limited exclusively to  $\gamma$ -rays. In principle, we need an efficiency factor that can extract only the  $\gamma$ -ray events. Such an efficiency factor is not provided in this analysis but should be derived and reported in the future by the experimental collaboration. It should be noted that this anisotropy would not be for the EBL, but the large event yield reduction is nevertheless striking.

The radial position of the Parker Solar Probe which orbits very close to the Sun's corona is around  $9.86 R_\odot$  from the solar centre [31]. Supposing EBL measurements could be performed in this orbit, excellent extraction of  $\gamma$ -ray suppression could be discerned. In the case of an orbit with similar radial position to the JWST, which is situated at the L2 Lagrange point, we would get a smaller EBL optical depth  $\tau_\gamma \simeq 1.5 \times 10^{-3}$  at  $E_\gamma = 1$  TeV. This is almost the same as on Earth, but if  $\gamma$ -rays are recorded at L2, the Earth's umbra would not interfere with the sunlight  $\gamma$ -ray interactions, which could provide a marginal improvement in the measurement.

For UHE neutrinos, in order to obtain optimistically large optical depths of  $\tau_\nu = 1 \times 10^{-16}\%$  at Earth and  $\tau_\nu = 2 \times 10^{-14}\%$  at the solar surface, we require energies of  $E_\nu = 4$  PeV. It is unlikely that such anisotropies will be probed with experiments such as IceCube which only have  $\mathcal{O}(1)$  event observations at PeV scale which is far too small to study such an anisotropy [32].

### IV. CONCLUSION

We consider suppression of diffuse extragalactic  $\gamma$ -rays and ultra-high-energy (UHE) neutrinos due to annihilation upon interactions with large numbers of photons and neutrinos emitted locally by the Sun. The annihilation induces anisotropies in the extragalactic background light (EBL) at 1 TeV with optical depths of  $\tau_\gamma \simeq 0.5\%$  and  $\tau_\gamma \simeq 2 \times 10^{-3}\%$  at the surface of the Sun and at Earth respectively. Such anisotropies are a direct prediction of Quantum Electrodynamics interactions and can potentially be probed with experiments such as Fermi LAT, H.E.S.S. and HAWC.

HAWC has measured dipole anisotropies of  $\simeq 10^{-2}\%$

due to cosmic rays travelling through the interstellar medium, and it has observed  $\gtrsim 3 \times 10^6$   $\gamma$ -ray events at  $\simeq 1$  TeV. If we consider the predicted optical depth of  $\simeq 2 \times 10^{-5}$  at Earth this suggests that potentially over  $\mathcal{O}(10^2)$   $\gamma$ -ray extragalactic photon events could be eradicated by sunlight. Maximal reduction of the EBL will occur when the EBL photons scatter directly against the solar photons at this energy. At energies much higher, the annihilation cross section falls off appreciably as does the EBL flux. Measurements of the TeV EBL suppression can be large around the Parker Solar Probe orbit  $\simeq 3.2 \times 10^{-2}\%$ , while for telescopes at L2 such as the JWST, the anisotropy is smaller around  $1.5 \times 10^{-3}\%$ . New experiments at these locations in the Solar System with  $\gamma$ -ray sensitivity could also probe EBL reduction.

In the case of ultra-high energy (UHE) neutrinos interacting with the solar neutrinos of average energy 0.53 MeV, we get much smaller optical depths. This is due to the smallness of the resonant and non-resonant contributions to the neutrino-antineutrino annihilation cross section. Even the most optimistic scenario can produce anisotropies of  $2 \times 10^{-14}\%$  and  $1 \times 10^{-16}\%$  for a PeV scale UHE neutrino scattering off 0.53 MeV solar neutrinos at the solar surface and at Earth respectively. Since experiments such as IceCube have only obtained a few PeV neutrino events, probing such a small anisotropy seems highly unrealistic with current experiments.

The result for diffuse  $\gamma$ -rays presents an optimal opportunity to study fundamental photon-photon interactions between isotropic background photons and thermal photons produced by the Sun in our neighbourhood of the universe. We do not study the effects on non-diffuse background contributions in detail, but the calculated optical depths may easily be applied to these scenarios as well.

## V. ACKNOWLEDGEMENTS

SB is supported by funding from the European Union's Horizon 2020 research and innovation programme under grant agreement No. 101002846 (ERC CoG "CosmoChart") as well as support from the Initiative Physique des Infinis (IPI), a research training program of the Idex SUPER at Sorbonne Université. SB would like to thank Maura E. Ramirez-Quezada and Yongchao Zhang for helpful discussions and feedback on the draft.

## VI. APPENDIX

The closed form solution for the resonant neutrino-antineutrino annihilation cross section in Eq.(3) is given

by

$$\sigma_{\nu\bar{\nu}}^R(p, k) = \frac{2\sqrt{2}G_F\Gamma m_Z}{2kE_{\nu\odot}} \left\{ \frac{1}{1+\xi} + \frac{m_Z^2}{4pk(1+\xi)^2} \log\left(\frac{f_+}{f_-}\right) + \frac{1-\xi}{(1+\xi)^2} \frac{m_Z^3}{4pk\Gamma} [\tan^{-1}(g_+) - \tan^{-1}(g_-)] \right\} \quad (11)$$

where  $\xi = \Gamma^2/m_Z^2$  and

$$f_{\pm} = 4k^2(1+\xi)(E_{\nu\odot} \pm p)^2 - 4m_Z^2k(E_{\nu\odot} \pm p) + m_Z^4$$

$$g_{\pm} = \frac{2k(1+\xi)(E_{\nu\odot} \pm p) - m_Z^2}{\Gamma m_Z} \quad (12)$$

---

\* sbalaji@lpthe.jussieu.fr

- [1] A. Lamastra, N. Menci, F. Fiore, L. A. Antonelli, S. Colafrancesco, D. Guetta, and A. Stamerra, *Astron. Astrophys.* **607**, A18 (2017), arXiv:1709.03497 [astro-ph.HE].
- [2] J. D. Finke, M. Ajello, A. Dominguez, A. Desai, D. H. Hartmann, V. S. Paliya, and A. Saldana-Lopez, (2022), arXiv:2210.01157 [astro-ph.GA].
- [3] E. Owen, A. Kong, and K.-G. Lee, *The extragalactic  $\gamma$ -ray background: imprints from the physical properties and evolution of star-forming galaxy populations* (2021).
- [4] A. Cooray, (2016), arXiv:1602.03512 [astro-ph.CO].
- [5] K. K. Singh, K. K. Yadav, and P. J. Meintjes, *Astrophys. Space Sci.* **366**, 51 (2021), arXiv:2105.14293 [astro-ph.CO].
- [6] Q. Yan-kun and Z. Hou-dun, *Chin. Astron. Astrophys.* **46**, 42 (2022).
- [7] K. Mattila and P. Väisänen, *Contemp. Phys.* **60**, 23 (2019), arXiv:1905.08825 [astro-ph.GA].
- [8] C. Lunardini, E. Sabancilar, and L. Yang, *JCAP* **08**, 014 (2013), arXiv:1306.1808 [astro-ph.HE].
- [9] S. E. Caddy, L. R. Spitler, and S. C. Ellis, arXiv preprint arXiv:2205.16002 (2022).
- [10] J. L. Bernal, A. Caputo, G. Sato-Polito, J. Mirocha, and M. Kamionkowski, (2022), arXiv:2208.13794 [astro-ph.CO].
- [11] J. C. D'Olivo, L. Nellen, S. Sahu, and V. Van Elewyck, *Astropart. Phys.* **25**, 47 (2006), arXiv:astro-ph/0507333.
- [12] R. Ruffini, G. V. Vereshchagin, and S. S. Xue, *Astrophys. Space Sci.* **361**, 82 (2016), arXiv:1503.07749 [astro-ph.HE].
- [13] A. Franceschini, *Universe* **7**, 146 (2021).
- [14] A. Nikishov, *Zhur. Eksptl'. i Teoret. Fiz.* **41** (1961).
- [15] G. G. Fazio and F. W. Stecker, *Nature* **226**, 135 (1970).
- [16] A. Loeb, *Res. Notes AAS* **6**, 148 (2022), arXiv:2207.00671 [hep-ph].
- [17] G. Breit and J. A. Wheeler, *Phys. Rev.* **46**, 1087 (1934).
- [18] R. J. Gould and G. P. Schröder, *Phys. Rev.* **155**, 1404 (1967).
- [19] R. Ruffini, G. Vereshchagin, and S.-S. Xue, *Phys. Rept.* **487**, 1 (2010), arXiv:0910.0974 [astro-ph.HE].
- [20] R. Brown, K. Mikaelian, and R. Gould, *Astrophysical Letters* **14**, 203 (1973).
- [21] P. A. Zyla *et al.* (Particle Data Group), *PTEP* **2020**, 083C01 (2020).

- [22] E. Roulet, Phys. Rev. D **47**, 5247 (1993).
- [23] G. Barenboim, O. Mena Requejo, and C. Quigg, Phys. Rev. D **71**, 083002 (2005), arXiv:hep-ph/0412122.
- [24] D. Lide, *CRC Handbook of Chemistry and Physics, 88th Edition* (Taylor & Francis, 2007).
- [25] A. Ianni, Phys. Dark Univ. **4**, 44 (2014).
- [26] M. Ackermann *et al.* (Fermi-LAT), Astrophys. J. **799**, 86 (2015), arXiv:1410.3696 [astro-ph.HE].
- [27] A. Abramowski *et al.* (H.E.S.S.), Astron. Astrophys. **550**, A4 (2013), arXiv:1212.3409 [astro-ph.HE].
- [28] A. Albert *et al.* (HAWC), Phys. Rev. D **98**, 123011 (2018), arXiv:1808.05620 [astro-ph.HE].
- [29] A. Kogut *et al.*, Astrophys. J. **419**, 1 (1993), arXiv:astro-ph/9312056.
- [30] A. U. Abeysekara *et al.* (HAWC, IceCube), Astrophys. J. **871**, 96 (2019), arXiv:1812.05682 [astro-ph.HE].
- [31] M. E. Wiedenbeck *et al.*, PoS **ICRC2017**, 016 (2018).
- [32] M. G. Aartsen *et al.* (IceCube), Phys. Rev. D **98**, 062003 (2018), arXiv:1807.01820 [astro-ph.HE].